IOP PUBLISHING JOURNAL OF PHYSICS A: MATHEMATICAL AND THEORETICAL

J. Phys. A: Math. Theor. **43** (2010) 235401 (11pp) doi:10.1088/1751-8113/43/23/235401

Motion of charged particles in a knotted electromagnetic field

M Arrayás and J L Trueba

Área de Electromagnetismo, Universidad Rey Juan Carlos, Camino del Molino s/n, 28943 Fuenlabrada, Madrid, Spain

E-mail: joseluis.trueba@urjc.es

Received 27 January 2010, in final form 25 March 2010
Published 13 May 2010
Online at stacks.iop.org/JPhysA/43/235401

Abstract

In this paper we consider the classical relativistic motion of charged particles in a knotted electromagnetic field. After reviewing how to construct electromagnetic knots from maps between the three-sphere and the two-sphere, we introduce a mean quadratic radius of the energy density distribution in order to study some properties of this field. We study the classical relativistic motion of electrons in the electromagnetic field of the Hopf map, and compute their trajectories. It is observed that these electrons initially at rest are strongly accelerated by the electromagnetic force, becoming ultrarelativistic in a period of time that depends on the knot energy and size.

PACS numbers: 03.50.De, 03.30.+p, 02.40.Pc

(Some figures in this article are in colour only in the electronic version)

1. Introduction

As pointed out in a recent paper by Irvine and Bouwmeester [1], electromagnetic knots are exact solutions of the classical Maxwell equations of electromagnetism in vacuum. They first appeared in a paper by Rañada [2] in 1989. Rañada himself [3] has used these solutions as the basic elements of a topological model of electromagnetism, which is locally equivalent to Maxwell's standard theory but implies furthermore some topological quantization conditions with interesting physical meaning [4–8].

Electromagnetic knots are defined through two fundamental complex scalar fields (ϕ, θ) whose level curves coincide with the magnetic and electric lines respectively, each one of these lines being labelled by the constant value of the corresponding scalar. Both scalars are assumed to have only one value at infinity, which is equivalent to compactifying the physical three-space to the sphere S^3. Moreover, the complex plane is compactified to the sphere S^2 via stereographic projection. As a result of such compactifications, the scalars ϕ and θ can be interpreted, at any time, as maps $S^3 \to S^2$, which can be characterized by the value of the Hopf index n [9]. It can be shown that the two scalar fields have the same Hopf index and

that the magnetic and the electric lines are generically linked with the same Gauss linking number ℓ. If μ is the multiplicity of the level curves (i.e. the number of different magnetic or electric lines that have the same label ϕ or θ), then the Hopf index of both scalars is $n = \ell\mu^2$. The Hopf index can thus be interpreted as a generalized linking number if we define a line as a level curve with μ disjoint components. Note that there are some cases of curves in R^3 in which the Gauss linking number is zero but the link is not topologically trivial. Examples are the Whitehead link or the Borromean rings [10]. These cases could be included in the model of electromagnetic knots provided the complex scalar fields can be found for these configurations.

An important feature of the model is that the Faraday 2-form $\mathcal{F} = \frac{1}{2}F_{\mu\nu}\,\mathrm{d}x^\mu \wedge \mathrm{d}x^\nu$ and its dual $*\mathcal{F} = \frac{1}{2}{}^*F_{\mu\nu}\,\mathrm{d}x^\mu \wedge \mathrm{d}x^\nu$ are proportional to the two pull-backs of σ, the area 2-form in S^2, by ϕ and θ,

$$\mathcal{F} = -\sqrt{a}\,\phi^*\sigma, \qquad *\mathcal{F} = c\sqrt{a}\,\theta^*\sigma, \tag{1}$$

where a is a constant introduced so that the magnetic and electric fields have correct dimensions and c is the velocity of light in vacuum. In the international system of units, a can be expressed as a pure number times the Planck constant $\hbar$ times the light velocity c times the vacuum permeability μ_0. As a consequence of the definitions (1), the maps ϕ and θ are dual to one another, $*(\phi^*\sigma) = -\theta^*\sigma$, where * is the Hodge or duality operator. This duality condition guarantees that both $\mathcal{F}$ and $*\mathcal{F}$ obey the Maxwell equations in empty space without the need of any other requirement.

The electromagnetic fields obtained in this way are called electromagnetic knots. They are radiation fields as they verify the condition $\mathbf{E}\cdot\mathbf{B} = 0$. It can be proved (see [5] for the details) that any radiation field in vacuum is locally equivalent to an electromagnetic knot. Moreover, because of the Darboux theorem, any electromagnetic field in empty space can be expressed locally as the sum of two radiation fields. Consequently, a model of electromagnetism based on these electromagnetic knots is locally equivalent to Maxwell standard theory. However, its difference from the global point of view has interesting consequences, as are the following topological quantizations. (i) The electric charge of any point particle must necessarily be equal to an integer multiple of the fundamental value $q_0 = \sqrt{\hbar c\epsilon_0}$ (see [6]). (ii) The electromagnetic helicity $\mathcal{H} = \hbar c(N_R - N_L)$ is also quantized [5], where N_R and N_L are the classical expressions of the number of right- and left-handed photons contained in the field (i.e. $N_R - N_L = \int \mathrm{d}^3k(\bar{a}_R a_R - \bar{a}_L a_L)$, $a_R(\mathbf{k})$, $a_L(\mathbf{k})$ being Fourier transforms of the vector potential A_μ in classical theory, but creation and annihilation operator in the quantum version). In fact, for any electromagnetic knot, $n = N_R - N_L$, which is a remarkable relation between the Hopf index (i.e. the generalized linking number) of the classical field and the classical case of the difference $N_R - N_L$. According to this relation, and taking into account the results of [11], adding a right or left photon would imply to add or remove a crossing of the field lines. (iii) The topology of the model also implies the quantization of the energy of the electromagnetic field in a cavity [7]. (iv) The magnetic flux of a superconducting ring is topologically quantized in the model of electromagnetic knots [8].

In this work we study a classical charged particle in a knotted electromagnetic field. We find that the particles can accelerate to the light velocity. We first revise the construction and some physical properties of the electromagnetic field built from the Hopf map between the compactified three-space (the sphere S^3) and the compactified complex plane (the sphere S^2). In particular, we pay attention to the electromagnetic energy density and how it evolves with time and introduce a mean quadratic radius of the energy density. Then we consider the relativistic motion of electrons in this electromagnetic field. We study the trajectories of the electrons and their velocities, showing that they become ultrarelativistic for a wide range of

the electromagnetic energy of the knot. Finally we give some conclusions and prospects of future work.

2. The electromagnetic field of the Hopf fibration

A method to find explicitly some electromagnetic knots can be found in [12]. Let $\phi_0(\mathbf{r})$, $\theta_0(\mathbf{r})$, be the two complex scalar fields such that they can be considered as maps $\phi_0, \theta_0 : S^3 \to S^2$ after identifying the physical space R^3 with S^3 and the complex plane with S^2. They have to satisfy the following two conditions.

Condition 1. The level curves of ϕ_0 must be orthogonal, at each point, to the level curves of θ_0, since we know that electromagnetic knots are radiation fields ($\mathbf{E}\cdot\mathbf{B} = 0$).

Condition 2. The Hopf index of ϕ_0 and of θ_0 are equal, $H(\phi_0) = H(\theta_0)$. This is necessary to ensure that the condition $\mathbf{E}\cdot\mathbf{B} = 0$ is maintained during time evolution.

Given ϕ_0 and θ_0 with these two conditions, we can construct the magnetic and electric fields at $t = 0$ as

$$\begin{aligned}\mathbf{B}(\mathbf{r},0) &= \frac{\sqrt{a}}{2\pi\,\mathrm{i}}\frac{\nabla\phi_0\times\nabla\bar{\phi}_0}{(1+\bar{\phi}_0\phi_0)^2},\\ \mathbf{E}(\mathbf{r},0) &= \frac{\sqrt{a}c}{2\pi\,\mathrm{i}}\frac{\nabla\bar{\theta}_0\times\nabla\theta_0}{(1+\bar{\theta}_0\theta_0)^2}.\end{aligned} \tag{2}$$

It is convenient to work with dimensionless coordinates in the mathematical spacetime $S^3\times R$, and in S^2. In order to do that, we define the dimensionless coordinates (X, Y, Z, T), related to the physical ones (x, y, z, t) (in the SI of units that we will use in this work) by

$$(X, Y, Z, T) = \frac{1}{L_0}(x, y, z, ct), \tag{3}$$

and $r^2/L_0^2 = (x^2+y^2+z^2)/L_0^2 = X^2+Y^2+Z^2 = R^2$, where L_0 is a constant with dimensions of length. Now, let us consider the Hopf map

$$\phi_0 = \frac{2(X+\mathrm{i}Y)}{2Z+\mathrm{i}(R^2-1)}, \tag{4}$$

whose fibres have been used as a basis for a case of knotted entanglement in reaction–diffusion models, in particular for a FitzHugh–Nagumo model [13]. We also consider the map corresponding to the change $(X, Y, Z) \mapsto (Y, Z, X)$ in (4):

$$\theta_0 = \frac{2(Y+\mathrm{i}Z)}{2X+\mathrm{i}(R^2-1)}. \tag{5}$$

Because of their construction, it is obvious that both maps (4) and (5) have the same Hopf index. In fact, these maps have Hopf index $n = 1$ and their fibrations are mutually orthogonal at each point. Consequently, we can build an electromagnetic knot from these maps. The Cauchy data for the magnetic and electric fields are

$$\begin{aligned}\mathbf{B}(\mathbf{r},0) &= \frac{8\sqrt{a}}{\pi L_0^2(1+R^2)^3}\left(Y-XZ, -X-YZ, \frac{-1-Z^2+X^2+Y^2}{2}\right),\\ \mathbf{E}(\mathbf{r},0) &= \frac{8\sqrt{a}c}{\pi L_0^2(1+R^2)^3}\left(\frac{1+X^2-Y^2-Z^2}{2}, -Z+XY, Y+XZ\right).\end{aligned} \tag{6}$$

Note that every time conditions 1 and 2 (see the beginning of this section) are necessary to construct electromagnetic fields in the form of equation (1). For example, take ϕ_0 as in

equation (4) but $\theta_0 = 0$. The fibres of these maps are obviously orthogonal at $t = 0$ but they have different Hopf indexes. When time evolves, the magnetic and electric fields will not be orthogonal.

From (6), two vector potentials $\mathbf{A}$ and $\mathbf{C}$ can be computed, such that $\mathbf{B} = \nabla \times \mathbf{A}$, $\mathbf{E} = \nabla \times \mathbf{C}$, with the results

$$\begin{aligned} \mathbf{A}(\mathbf{r}, 0) &= \frac{2\sqrt{a}}{\pi L_0 (1+R^2)^2}(Y, -X, -1), \\ \mathbf{C}(\mathbf{r}, 0) &= \frac{2\sqrt{a}c}{\pi L_0 (1+R^2)^2}(1, -Z, Y). \end{aligned} \tag{7}$$

The magnetic and electric helicities of this knot are defined to be

$$\begin{aligned} h_m &= \frac{1}{2\mu_0}\int_{R^3} \mathbf{A}\cdot\mathbf{B}\,\mathrm{d}^3 r, \\ h_e &= \frac{\varepsilon_0}{2}\int_{R^3} \mathbf{C}\cdot\mathbf{E}\,\mathrm{d}^3 r, \end{aligned} \tag{8}$$

where ε_0 is the vacuum permittivity. Taking into account the Cauchy data (6) and the potentials (7), the electromagnetic helicity yields

$$h = h_m + h_e = \frac{a}{2\mu_0} + \frac{a}{2\mu_0} = \frac{a}{\mu_0}. \tag{9}$$

To find the electromagnetic knot at any time from the Cauchy data (6), we use Fourier analysis. The fields turn out to be [12]

$$\begin{aligned} \mathbf{B}(\mathbf{r}, t) &= \frac{\sqrt{a}}{\pi L_0^2 (A^2+T^2)^3}(Q\mathbf{H}_1 + P\mathbf{H}_2), \\ \mathbf{E}(\mathbf{r}, t) &= \frac{\sqrt{a}c}{\pi L_0^2 (A^2+T^2)^3}(Q\mathbf{H}_2 - P\mathbf{H}_1), \end{aligned} \tag{10}$$

where the quantities A, P, Q are defined by

$$A = \frac{R^2 - T^2 + 1}{2}, \qquad P = T(T^2 - 3A^2), \qquad Q = A(A^2 - 3T^2), \tag{11}$$

and the vectors $\mathbf{H}_1$ and $\mathbf{H}_2$ are

$$\begin{aligned} \mathbf{H}_1 &= \left(Y + T - XZ, -X - (Y+T)Z, \frac{-1 - Z^2 + X^2 + (Y+T)^2}{2}\right), \\ \mathbf{H}_2 &= \left(\frac{1 + X^2 + Z^2 - (Y+T)^2}{2}, -Z + X(Y+T), Y + T + XZ\right). \end{aligned} \tag{12}$$

This solution now fulfils $\mathbf{E}\cdot\mathbf{B} = 0$ and $E^2 - c^2 B^2 = 0$ at any time. It is possible to obtain directly the electromagnetic field (10) from the time-dependent expressions (1). In terms of the magnetic and the electric fields, we have

$$\begin{aligned} \mathbf{B}(\mathbf{r}, t) &= \frac{\sqrt{a}}{2\pi \mathrm{i}(1+\phi\bar{\phi})^2}\nabla\phi \times \nabla\bar{\phi} = \frac{\sqrt{a}}{2\pi \mathrm{i}c(1+\theta\bar{\theta})^2}\left(\frac{\partial\bar{\theta}}{\partial t}\nabla\theta - \frac{\partial\theta}{\partial t}\nabla\bar{\theta}\right), \\ \mathbf{E}(\mathbf{r}, t) &= \frac{\sqrt{a}c}{2\pi \mathrm{i}(1+\theta\bar{\theta})^2}\nabla\bar{\theta} \times \nabla\theta = \frac{\sqrt{a}}{2\pi \mathrm{i}(1+\phi\bar{\phi})^2}\left(\frac{\partial\bar{\phi}}{\partial t}\nabla\phi - \frac{\partial\phi}{\partial t}\nabla\bar{\phi}\right), \end{aligned} \tag{13}$$

where the time-dependent expressions of the maps ϕ and θ are (see [5])

$$\begin{aligned} \phi &= \frac{(AX - TZ) + \mathrm{i}(AY + T(A-1))}{(AZ + TX) + \mathrm{i}(A(A-1) - TY)}, \\ \theta &= \frac{(AY + T(A-1)) + \mathrm{i}(AZ + TX)}{(AX - TZ) + \mathrm{i}(A(A-1) - TY)}. \end{aligned} \tag{14}$$

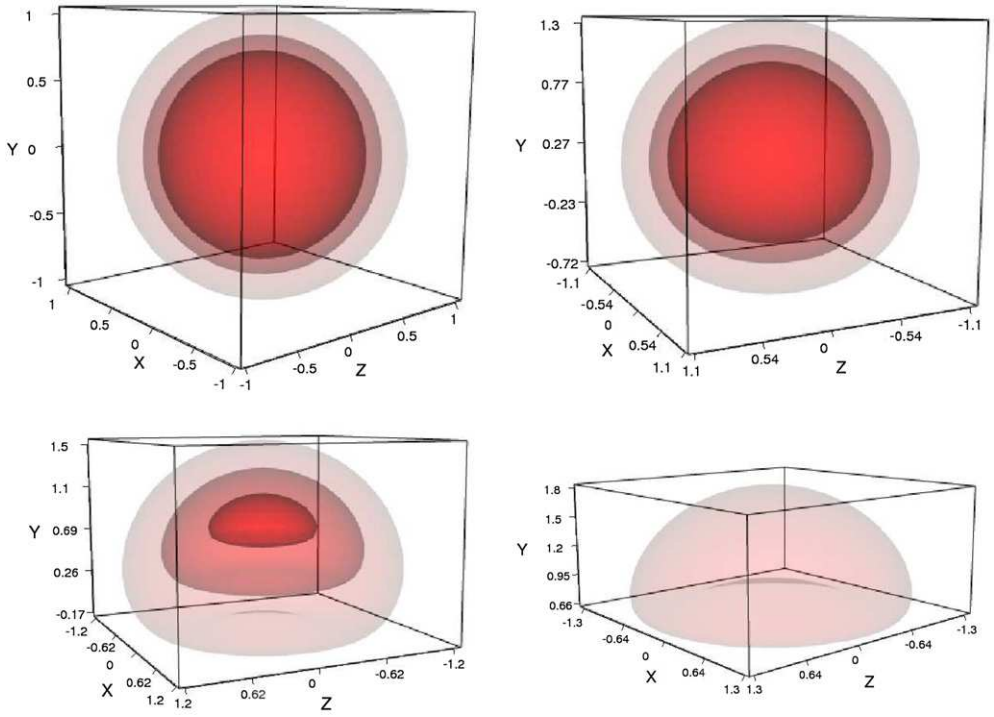

Figure 1. Evolution of three energy density levels of the electromagnetic knot of the Hopf fibration. From left to right and top to bottom, $T = 0$, $T = 0.5$, $T = 1$, $T = 1.5$. Coordinates (X, Y, Z) are dimensionless and are related to the physical coordinates (x, y, z) through $(X, Y, Z) = (x, y, z)/L_0$. The levels correspond to values 0.1, 0.2 and 0.3 of the density energy in $a/(\mu_0 L_0^4)$ units (see equation (15)). The density energy levels displayed are 0.1, 0.2 and 0.3 in increasing order of colour intensity. At $T = 1.5$, the levels 0.2 and 0.3 are not present.

Note that the level curves of both maps ϕ and θ remain linked with a Gauss linking number equal to 1. The evolution of the curved lines of these maps gives the evolution of the force lines of the magnetic and electric fields given by the expressions (13).

The energy density of the electromagnetic field (10) is given by,

$$U(\mathbf{r}, t) = \frac{\varepsilon_0 E^2}{2} + \frac{B^2}{2\mu_0} = \frac{a}{4\pi^2 \mu_0 L_0^4} \frac{(1 + X^2 + (Y + T)^2 + Z^2)^2}{(A^2 + T^2)^3}. \tag{15}$$

The maximum of the energy density is located at $X = Z = 0$ during time evolution. The function U is symmetric in the coordinates X and Z. In figure 1, we show some isosurfaces of the energy density U for times $T = 0, 0.5, 1, 1.5$. The energy density levels represented are 0.1, 0.2 and 0.3 in $a/(\mu_0 L_0^4)$ units. It can be seen how the isosurfaces spread as the energy density goes to zero. For time $T = 1.5$, the 0.3 and 0.2 levels have disappeared. Note that the total electromagnetic energy of the knot

$$\mathcal{E} = \int U \, \mathrm{d}^3 r = \frac{2a}{\mu_0 L_0} \tag{16}$$

remains constant. Note that the same helicity unit a also appears in the energy of the electromagnetic knot. Relations between topology and energy of magnetic knots have been studied recently in [14].

At $T = 0$, the energy density has spherical symmetry and its maximum is located at the origin. As time increases, the symmetry is broken and the maximum is located at $X = Z = 0$ and Y close to T. Approximately, the position of the maximum of the energy density can be found up to $T = 1$ at $X = Z = 0$, $Y = T(1 + 6T^2)/(2 + 6T^2)$.

The energy density of the knot extends to infinity, but we can define a mean quadratic radius of the energy distribution as

$$\langle r^2 \rangle = \frac{\int (\mathbf{r} - \mathbf{r}_{\max})^2 U \, \mathrm{d}^3 r}{\int U \, \mathrm{d}^3 r}, \tag{17}$$

where $\mathbf{r}_{\max}$ is the position of the maximum of the distribution. At $T = 0$, the distribution has spherical symmetry and the mean quadratic radius of the distribution is given by $\sqrt{\langle r^2 \rangle} = L_0$. The maximum has a value of the (dimensionless) energy density equal to $16/\pi^2$ and at a distance equal to the mean quadratic value, the dimensionless energy density is $1/\pi^2$. This means that, initially, more than 70% of the energy is localized inside a sphere of radius L_0 centred at the origin. As time evolves the mean quadratic radius of the distribution spreads out (its value at $t = L_0/c$ or $T = 1$ is about $1.1\, L_0$) and the position of the centre is at $(0, 7/8, 0)$. Note that the distribution is not well characterized as a sphere as time evolves.

One can also compute the Poynting vector $\mathbf{P}$ of the electromagnetic field, obtaining

$$\mathbf{P} = \int \frac{\mathbf{E} \times \mathbf{B}}{\mu_0} \, \mathrm{d}^3 r = \left(0, \frac{ac}{2\mu_0 L_0}, 0\right). \tag{18}$$

As can be seen, it has a single contribution along the y-axis. This explains why the maximum of the energy density moves along this axis for the electromagnetic knot studied in this paper.

3. Relativistic motion of charges in the electromagnetic knot of the Hopf fibration

Now we apply the electromagnetic knot studied in the previous section to the following situation. Suppose that this knot has been created in certain region of the space, so we have at $t = 0$ a knot initially centred at the origin, that moves with time along the y-axis as we discussed in the previous section. Let us assume there are free electrons with negligible initial velocities in units of the light velocity c. We consider the evolution of these electrons under the electromagnetic knot field.

The velocity of the electrons increases by the action of the electromagnetic field, so we will solve the relativistic equation for the motion of single electrons [15], considered as test particles which do not affect the value of the electromagnetic field obtained from the Hopf fibration. The equation to be considered is

$$\frac{\mathrm{d}\mathbf{v}}{\mathrm{d}t} = -\frac{e}{m}\sqrt{1 - \frac{v^2}{c^2}} \left(\mathbf{E} + \mathbf{v} \times \mathbf{B} - \frac{1}{c^2}\mathbf{v}(\mathbf{v} \cdot \mathbf{E})\right), \tag{19}$$

where $e = 1.6 \times 10^{-19}$ C is the electron charge, and $m = 9.1 \times 10^{-31}$ kg is its rest mass. Using dimensionless quantities and expressions (10) for the electromagnetic knot of the Hopf fibration, we find

$$\frac{\mathrm{d}\mathbf{V}}{\mathrm{d}T} = -\frac{e\sqrt{a}}{\pi m c L_0} \frac{\sqrt{1 - V^2}}{(A^2 + T^2)^3} \cdot (Q\mathbf{H}_2 - P\mathbf{H}_1 + \mathbf{V} \times (Q\mathbf{H}_1 + P\mathbf{H}_2) - \mathbf{V}(\mathbf{V} \cdot (Q\mathbf{H}_2 - P\mathbf{H}_1)). \tag{20}$$

Different possible physical situations can be studied with equation (20) by changing the value of the dimensionless term $g = e\sqrt{a}/(\pi m c L_0)$. For electrons, taking into account that the total

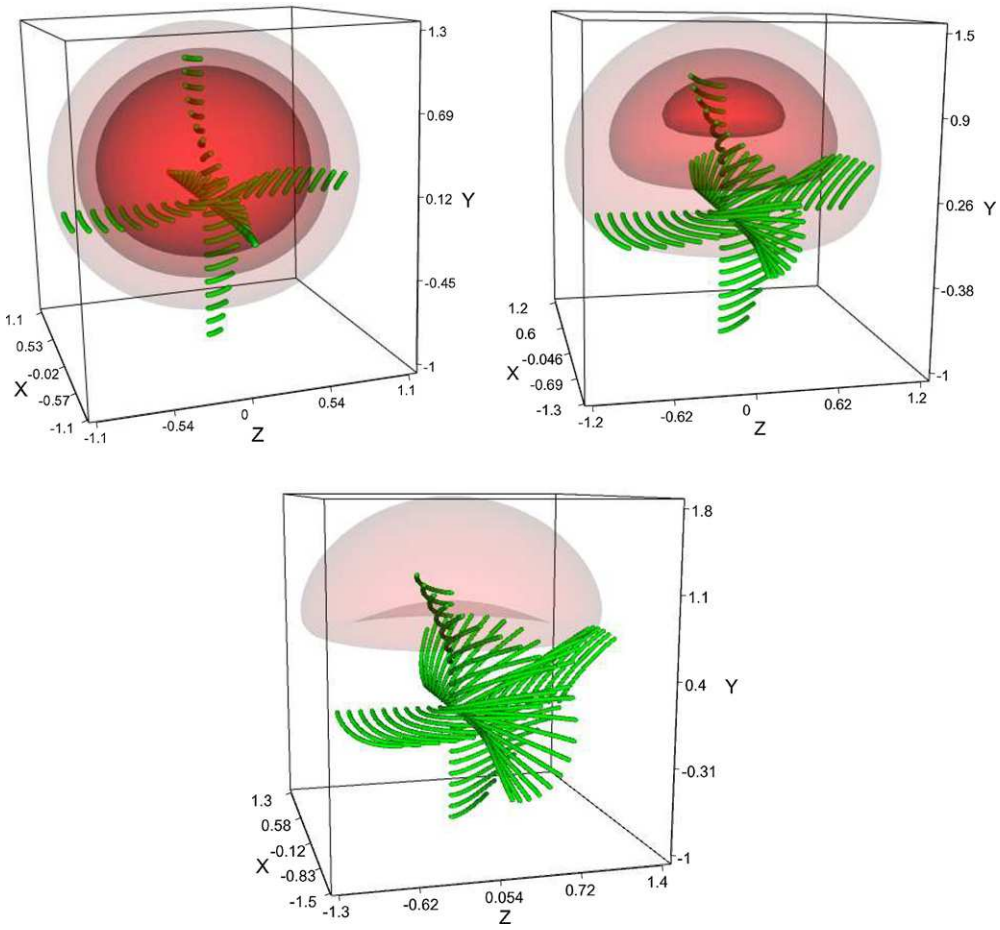

Figure 2. Evolution of the position of electrons under the influence of the electromagnetic knot of the Hopf fibration with $g = 1$. From left to right and top to bottom, $T = 0.5$, $T = 1$, $T = 1.5$. The energy levels shown correspond to values 0.1, 0.2 and 0.3 of the density energy in $a/(\mu_0 L_0^4)$ for the same times (see figure 1). The initial velocity of the electrons is $V_0 = 0$. The electron initial positions considered are given by $\mathbf{R}_0 = (R_i, 0, 0)$, with $R_i = \pm 0.1, \pm 0.2, \ldots, \pm 1$, by $\mathbf{R}_0 = (0, R_i, 0)$, and by $\mathbf{R}_0 = (0, 0, R_i)$. After $T = 1.5$ these electrons move almost freely. The final values of the velocities at $T = 1.5$ run from $V_{\min} = 0.5300$ to $V_{\max} = 0.8410$ in units of the light velocity c.

energy of the field is $\mathcal{E} = 2a/(\mu_0 L_0)$ and that the size of the knot is characterized initially by L_0, the term in equation (20) can be written as

$$g = \frac{e\sqrt{a}}{\pi m c L_0} \approx 0.15 \sqrt{\frac{\mathcal{E}}{L_0}}, \tag{21}$$

where $\mathcal{E}$ is measured in Joules and L_0 in metres.

In figure 2, the evolution of the position of electrons can be seen when $g = 1$. The initial velocity of the electrons is $V_0 = 0$. We have taken for these electrons initial positions along the x-, y- and Z-axis. In each axis, the dimensionless position is $\pm 0.1, \pm 0.2, \ldots \pm 1$. In the figure, the electron trajectories are plotted from $T = 0$ up to $T = 0.5$ (top left), up to $T = 1$ (top right) and up to $T = 1.5$ (bottom). We also include some energy density

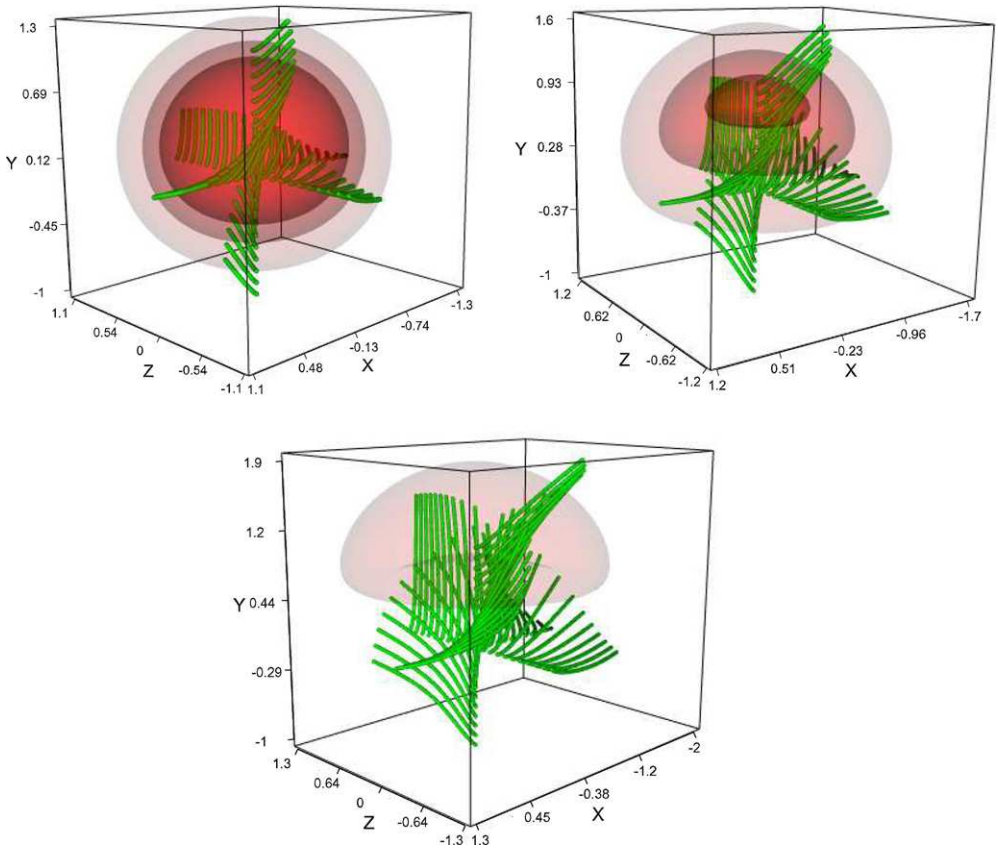

Figure 3. Same situation as in figure 2 with a value $g = 10$. From left to right and top to bottom, $T = 0.5$, $T = 1$, $T = 1.5$. The energy levels shown correspond to values 0.1, 0.2 and 0.3 of the density energy in $a/(\mu_0 L_0^4)$ for the same times (see figure 1). The initial velocity of the electrons is $V_0 = 0$. The electron initial positions considered are given by $\mathbf{R}_0 = (R_i, 0, 0)$, with $R_i = \pm 0.1, \pm 0.2, \ldots, \pm 1$, by $\mathbf{R}_0 = (0, R_i, 0)$, and by $\mathbf{R}_0 = (0, 0, R_i)$. The final values of the velocities at $T = 1.5$ run from $V_{\min} = 0.9684$ to $V_{\max} = 0.9942$ in units of the light velocity c.

levels of the electromagnetic knot at the time considered, corresponding to values 0.1, 0.2 and 0.3 in $a/(\mu_0 L_0^4)$ units (see the caption of figure 1 for more details). By doing so, in figure 2 we see not only the evolution of the position of some free electrons, but also the region in which the interaction with the electromagnetic knot (whose centre moves along the y-axis with a velocity close to c) is more important. This fact explains some features of the behaviour of the electron trajectories. At the beginning, up to $T = 0.5$, the region where the electrons are is influenced by the high values of the knot energy density, so that the electrons are accelerated and their trajectories are curved by the influence of the electromagnetic force. From $T = 0.5$ up to $T = 1$, the centre of the knot has moved along the y-axis and many electrons are now in a region where the electromagnetic density is smaller. However, the electromagnetic force is still important so that many electrons tend to follow the motion of the centre of the knot (a small fraction of the electrons seem to be curved towards the opposite direction). This is also the situation from $T = 1$ up to $T = 1.5$, during which electrons reach high values of the velocity, in the range from $V_{\min} = 0.5300$ to $V_{\max} = 0.8410$ in units of the light velocity c. After this time, the influence of the electromagnetic knot on the electron trajectories is smaller, and they can be considered as almost free.

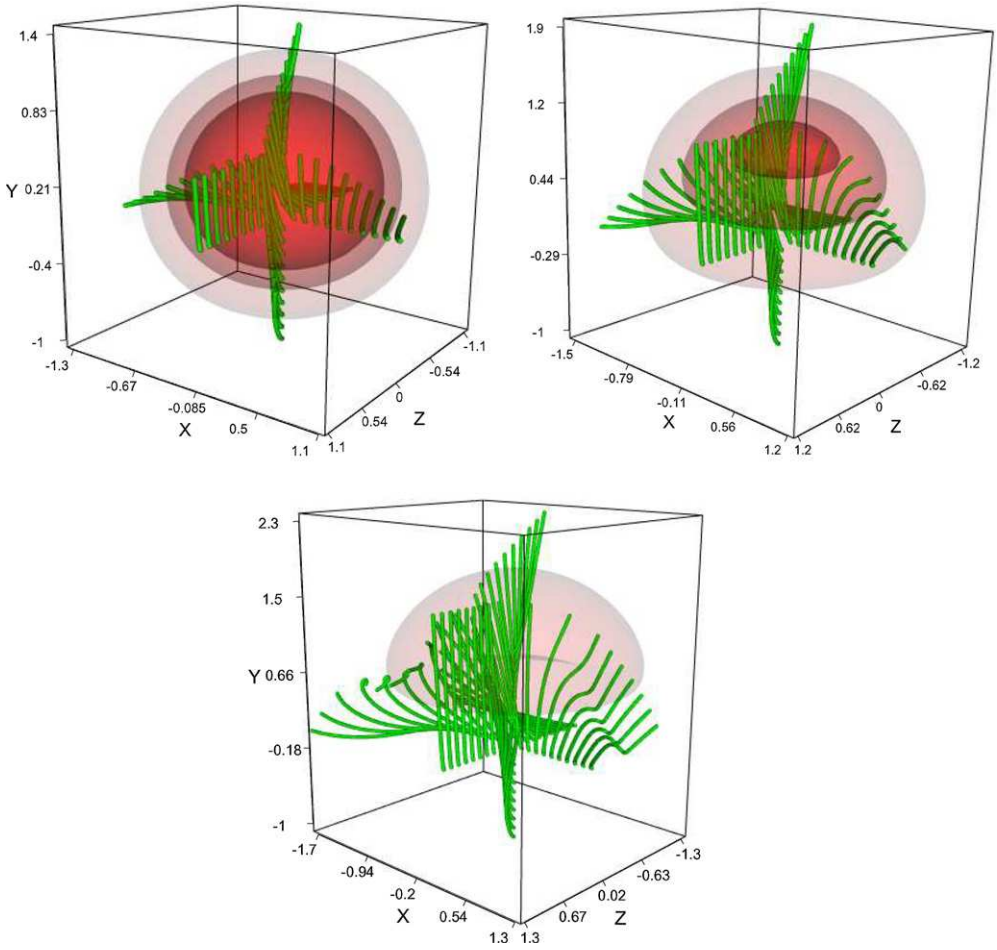

Figure 4. Same situation as in figures 2 and 3 with a value $g = 100$. From left to right and top to bottom, $T = 0.5$, $T = 1$, $T = 1.5$. The energy levels shown correspond to values 0.1, 0.2 and 0.3 of the density energy in $a/(\mu_0 L_0^4)$ for the same times. The initial velocity of the electrons is $V_0 = 0$. The electron initial positions considered are given by $\mathbf{R}_0 = (R_i, 0, 0)$, with $R_i = \pm 0.1, \pm 0.2, \ldots, \pm 1$, by $\mathbf{R}_0 = (0, R_i, 0)$, and by $\mathbf{R}_0 = (0, 0, R_i)$. The final values of the velocities at $T = 1.5$ run from $V_{\min} = 0.9870$ to $V_{\max} = 0.9999$ in units of the light velocity c.

In figure 3, the evolution of the position of electrons is studied when $g = 10$. The initial velocity of the electrons is $V_0 = 0$, and the initial positions in each axis are given by $\pm 0.1, \pm 0.2, \ldots \pm 1$ in units of the knot size L_0 as before. As in figure 2, the electron trajectories are plotted in figure 3 from $T = 0$ up to $T = 0.5$ (top left), up to $T = 1$ (top right) and up to $T = 1.5$ (bottom), and we include some energy density levels of the electromagnetic knot at the time considered, corresponding to the values 0.1, 0.2 and 0.3 in $a/(\mu_0 L_0^4)$ units. Up to $T = 0.5$, the electrons get higher acceleration and their trajectories are more curved by the influence of the electromagnetic force than in the case of $g = 1$ (figure 2). From $T = 0.5$ up to $T = 1$, all the electrons tend to follow the motion of the centre of the knot, a situation much clearer from $T = 1$ up to $T = 1.5$. The final velocities of these electrons are in the range from $V_{\min} = 0.9684$ to $V_{\max} = 0.9942$ in units of the light velocity c.

In figure 4, the evolution of the position of electrons can be seen when $g = 100$. The initial velocity and initial position of the electrons are the same as in the cases $g = 1$ (figure 2) and $g = 10$ (figure 3). As in previous cases, electron trajectories are plotted in figure 4 from $T = 0$ up to $T = 0.5$ (top left), up to $T = 1$ (bottom) and up to $T = 1.5$ (top right), and we include some energy density levels of the electromagnetic knot at the time considered, corresponding to values 0.1, 0.2 and 0.3 in $a/(\mu_0 L_0^4)$ units. The global behaviour of the electron trajectories is very similar to the case in which $g = 10$, but now the electrons are even more accelerated and their trajectories are even more curved by the influence of the electromagnetic force. All the electrons clearly tend to follow the motion of the centre of the knot along the y-axis, with final velocities in the range from $V_{\min} = 0.9870$ to $V_{\max} = 0.9999$ in units of the light velocity c.

4. Conclusions

In this paper we have considered the classical relativistic motion of charged particles in a knotted electromagnetic field. We have seen how to construct electromagnetic knots from maps between the three-sphere and the two-sphere. In the particular case of the Hopf map, whose fibres are mutually linked, we have written the expression for the electromagnetic field. This is a solution of the Maxwell equations in vacuum, such that any pair of electric lines is a link and any pair of magnetic lines is a link. We have considered some properties of this field, in particular the electromagnetic energy density. We have seen that a major part of the energy density of the knot is, at $t = 0$, localized into a sphere whose radius is the mean quadratic radius of the energy density distribution. As time evolves, the spherical symmetry is broken and the mean quadratic radius of the distributions spreads out.

We have considered the relativistic motion of electrons (considered as point particles) in the electromagnetic field of the Hopf map. We have computed the trajectories of the electrons starting with zero initial velocities, and we have seen that these electrons are strongly accelerated by the electromagnetic force, becoming ultrarelativistic in a period of time that depends on the knot size.

Finally we consider that a deeper understanding of the interaction between electromagnetic knots and test particles could be useful to design experiments to produce knots in the laboratory.

Acknowledgment

The authors thank the Spanish Ministerio de Educación y Ciencia for support under project AYA2009-14027-C07-04.

References

[1] Irvine W T M and Bouwmeester D 2008 *Nature Phys.* **4** 716–20
[2] Rañada A F 1989 *Lett. Math. Phys.* **18** 97–106
[3] Rañada A F 1992 *J. Phys. A: Math. Gen.* **25** 1621–41
[4] Rañada A F and Trueba J L 1995 *Phys. Lett.* A **202** 337–42
[5] Rañada A F and Trueba J L 1997 *Phys. Lett.* A **232** 25–33
[6] Rañada A F and Trueba J L 1998 *Phys. Lett.* B **422** 196–200
[7] Rañada A F 2003 *Phys. Lett.* A **310** 434–44
[8] Rañada A F and Trueba J L 2006 *Found. Phys.* **36** 427–36
[9] Hopf H 1931 *Math. Ann.* **104** 637–65
[10] Marsh G 1996 *Force-Free Magnetic Fields: Solutions, Topology and Applications* (Singapore: World Scientific)

[11] Moffatt H K and Ricca R L 1992 *Proc. R. Soc. Lond.* A **439** 411–29
[12] Rañada A F and Trueba J L 2001 *Modern Nonlinear Optics. Part III* ed M Evans (New York: Wiley) pp 197–254
[13] Trueba J L and Arrayás M 2009 *J. Phys. A: Math. Theor.* **42** 282001
[14] Ricca R L 2008 *Proc. R. Soc.* A **464** 293–300
[15] Landau L D and Lifshitz E M 1975 *The Classical Theory of Fields* 4th edn (Amsterdam: Elsevier)